SERBIAN JOURNAL OF ELECTRICAL ENGINEERING
Vol. 2, No. 2, November 2005, 147 - 156

Shielding Effect of Non -Ferrous Metallic Plates in Vicinity of Three Phase Conductors

Miodrag Milutinov[1], Neda Pekarić-Nađ[2]

Abstract: This paper uses multi conductor based method (MCM) for numerical estimation of magnetic field cancellation around balanced three phase power conductors introduced by aluminum plates. Aluminum was identified as a suitable shielding material for moderate field reduction due to its low cost and satisfactory shielding performance.

Keywords: Electromagnetic compatibility, Shielding, Field cancellation

1 Introduction

Power frequency (50/60Hz) magnetic fields can have unacceptable levels in households and offices and affect electronic devices and humans. If necessary, the fields may be reduced to acceptable levels by shielding. μ-Metal (ferromagnetic) shields are well known but expansive. "Magnetic fields are shielded at DC and ELF level only by providing a low reluctance path as an alternative for the incident magnetic field" [1]. The aim of this work was to explore the other options. More precisely, can affordable shields be made of thick conductive material such as aluminum? In the case of extremely low frequencies (ELF 3 Hz – 3 kHz), eddy currents induced in metallic plates may become relevant. In this case the shielding effect of some nonferrous metallic structures can be as good as for a ferromagnetic structure.

This paper explores a possibility and effectiveness of protection by non-ferrous high conductivity structures - such as thick aluminum plates. The ferrous structures, such as thick iron plates, are explored for the sake of completeness.

1.1 Shielding by increased conductivity material

Protection mechanism of a good conductivity material is based on induced eddy currents. The field reduction comes as a result of eddy currents induced in

[1]University of Novi Sad, FTN, Electrical Engineering, Trg Dositeja Obradovica 6, 21000 Novi Sad, Serbia&Montenegro, E-mail: miodragm@uns.ns.ac.yu
[2]University of New Hampshire, Kingsbury Hall, Durham NH 03824, USA, E-mail: nnad@unh.edu
[*]This work was completed under project "Modeling of the Electromagnetic Fields in Electro-distributive Systems", financed by the Ministry of Science, Technology and Development, Republic of Serbia.

the plates according to Faraday's Law of Induction (See Fig. 1). Eddy currents are generated when incident EM field illuminates good conductor. The eddy currents generate magnetic field that opposes the original field, resulting in reduction of the magnetic field. It is important to note that the "eddy current cancellation" mechanism depends on the frequency.

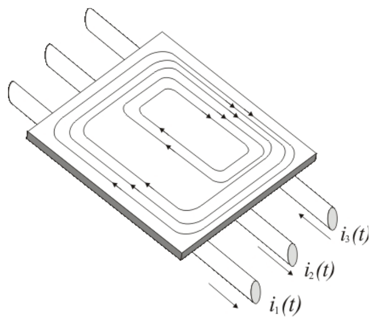

Fig. 1 – *Eddy currents induced in a metal plate by balanced three phase conductors.*

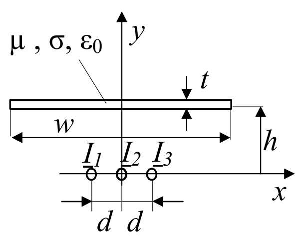

Fig. 2 – *Balanced three phase system and the shield of thickness t, width w and height h.*

1.2 Shielding by increased permeability material

A costly high permeability material provides shielding by mechanism called "flux shunting". In this case magnetic flux from a source is diverted into the magnetic material and away from the region to be shielded.

2 Theoretical Basis

Electromagnetic field satisfies Maxwell’s equations [2],

$$\oint_C \boldsymbol{E}\,\mathrm{d}\boldsymbol{l} = -\int_S \frac{\partial \boldsymbol{B}}{\partial t}\,\mathrm{d}\boldsymbol{S}\,, \tag{1}$$

$$\oint_C \boldsymbol{H}\,\mathrm{d}\boldsymbol{l} = \int_S \left(\boldsymbol{J} + \frac{\partial \boldsymbol{D}}{\partial t}\right)\mathrm{d}\boldsymbol{S}\,, \tag{2}$$

$$\oint_S \boldsymbol{B}\,\mathrm{d}\boldsymbol{S} = 0 . \tag{3}$$

The geometry examined in this work is presented in Fig. 2. The currents of the power conductors are assumed to be time harmonic, with a 10A amplitude. The separation between the copper conductors was taken to be 10cm. The shield was of width $w = 80\,\mathrm{cm}$, overall thickness *t* and distance *h* from the conductors. The electrical constants used to characterize the shields are free space permeability μ_0 or iron permeability, $\mu_r = 100$, aluminum conductivity $\sigma = 37\times10^6\,\mathrm{S}$, iron conductivity $\sigma = 10\times10^6\,\mathrm{S}$, and free space permittivity, ε_0.

As the measurement results were not available, two methods were used in order to verify the results: Multi Conductor Method (MCM) [3] and Finite Element Method (FEM) [4]. The MCM was used to estimate magnetic flux density in the case of non-ferrous plates. Since the MCM uses equations with mutual inductance, the method could not be applied to ferromagnetic shields. Because of that the FEM was used to estimate magnetic flux density around ferrous plates. The FEM was also used to verify the MCM method in the case of non-ferrous plates.

2.1 Multi Conductor Method

The Multi Conductor Method, MCM, can be applied if the plate is long enough and can be divided into *n* parallel sub-conductors, as shown in Fig. 3a. The voltage drop in the shield and the voltage drop in the current carrying conductors can be estimated using the voltage definition,

$$\begin{bmatrix} [\underline{U}_\mathrm{s}]_{1\times n} \\ [\underline{U}_\mathrm{c}]_{1\times k} \end{bmatrix} = \begin{bmatrix} [\underline{Z}_\mathrm{ss}]_{n\times n} & [\underline{Z}_\mathrm{sc}]_{n\times k} \\ [\underline{Z}_\mathrm{cs}]_{k\times n} & [\underline{Z}_\mathrm{cc}]_{k\times k} \end{bmatrix} \begin{bmatrix} [\underline{I}_\mathrm{s}]_{1\times n} \\ [\underline{I}_\mathrm{c}]_{1\times k} \end{bmatrix} . \tag{4}$$

The $[\underline{U}_\mathrm{s}]_{1\times n}$ and $[\underline{U}_\mathrm{c}]_{1\times k}$ are the voltage drops in the shield and in the conductors, $[\underline{Z}_\mathrm{ss}]_{n\times n}$ and $[\underline{Z}_\mathrm{cc}]_{k\times k}$ are the shield and the conductors related matrices and $[\underline{Z}_\mathrm{sc}]_{n\times k}$ and $[\underline{Z}_\mathrm{cs}]_{k\times n}$ represent the matrices of mutual inductance between sub-conductors and the current carrying conductors. Vector $[\underline{I}_\mathrm{s}]_{1\times n}$ is the vector of induced eddy currents in the shield and $[\underline{I}_\mathrm{c}]_{1\times k}$ is the vector of currents in the power conductors. The shield is assumed isolated, so

$$\sum_1^n \underline{I}_S = 0 . \tag{5}$$

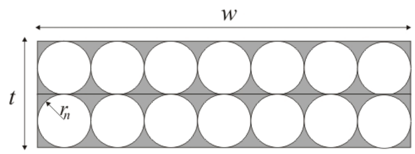

Fig. 3a – *The cross section of the shield substitution for MCM.*

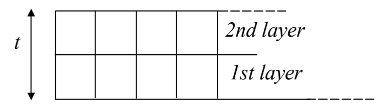

Fig. 3b – *Mesh-model of the shield for FEM.*

2.2 Finite Element Method

The FEM is based on magnetic vector potential equation derived from Maxwell's equations (1) and (2) as

$$\Delta \underline{\boldsymbol{A}} - \varepsilon\mu \frac{\partial^2 \underline{\boldsymbol{A}}}{\partial t^2} = -\mu \underline{\boldsymbol{J}} \,. \tag{6}$$

Because of the steady state harmonic analysis assumed in this work, complex formulation is used. Penetration depth for aluminum plate at the power frequency (50/60 Hz) and conductivity of $37\times10^6\,\mathrm{S}$ is $11\,\mathrm{mm}$. For an iron plate the penetration depth depends on permeability. It is approximately $2\,\mathrm{mm}$ at $\mu_r = 100$ and $1\,\mathrm{mm}$ at $\mu_r = 1000$. Separation between the two neighboring nodes in the mesh model of the shield needs to be less than one half of the penetration depth. For aluminum shield it needs to be less than $5\,\mathrm{mm}$. For the iron shields it needs to be less than 1mm and $0.5\,\mathrm{mm}$ respectively. Most often, several layers need to be introduced as shown in Fig. 3b.

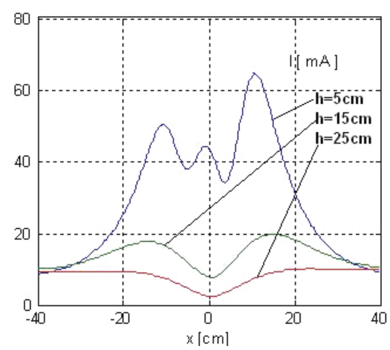

Fig. 4a – *Induced current density of the aluminum shield found by the MCM (t=2mm, w=80cm, h=5,15,25 cm): direct sequence currents in the power conductors.*

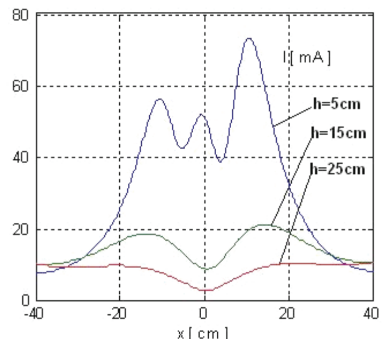

Fig. 4b – *Induced current density of the aluminum shield found by the FEM (t=2mm, w=80cm, h=5,15,25 cm): direct sequence currents in the power conductors.*

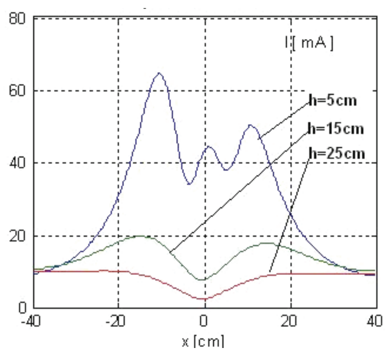

Fig. 4c – *Induced current density of the aluminum shield found by MCM (t=2mm, w=80cm, h=5,15,25 cm): reverse sequence currents in the power conductors.*

3 Results of the Calculations

There are three conductors to be shielded in the case of a balanced three-phase system. Direct sequence currents were assumed with the 0º, -120º and -240º phase shift respectively. Calculation of the resulting EM field very close to the conductors is quite complex, due to the elliptic polarization of the EM field in proximity of the conductors. For the geometry from Fig. 2 the polarization of the EM field is approximately linear outside the cylinder of diameter 4*d,* having middle conductor along its axes.

The accuracy of the MCM solution was tested by the FEM in the case of t=2mm thick aluminum shield. A good agreement was found as can be concluded from Figs. 4a and 4b. The two sets of results were found to be slightly different due to the different approximation of the shield's geometry (Fig. 3a). In the worst case the magnitudes differ by factor of 1.27, the same factor that relates the rectangular area (for the FEM calculations) and its approximation by a number of circles (in the case of the MCM calculations). The difference was more pronounced when the shield was closer (h=5cm) and less when the shield was away from the conductors. The solutions are considered to be in a good agreement, as can be seen from Figs. 4a and 4b.

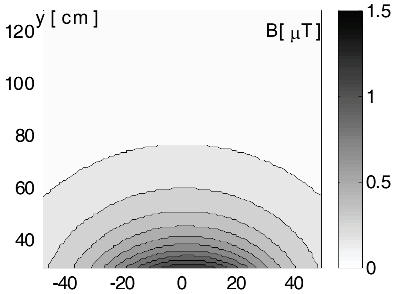

a1) Aluminum, h = 5 cm

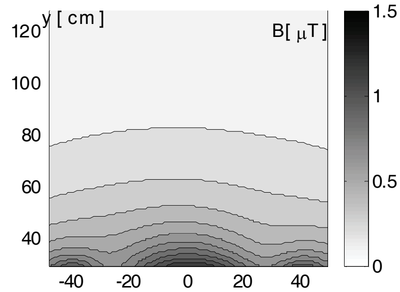

b1) Aluminum, h = 25 cm

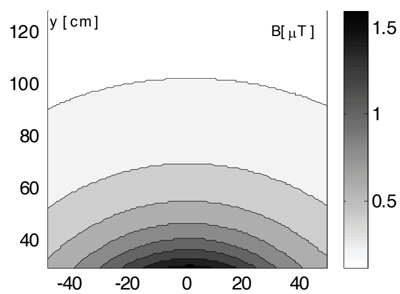

a2) Iron, h = 5 cm

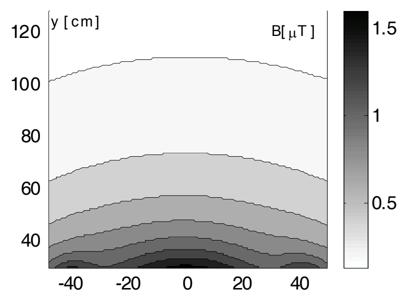

b2) Iron, h = 25 cm

Fig. 5 – *Vector B magnitude in the area of interest, starting 30 cm above the three phase conductors for the different shield heights h; Aluminum and Iron shields, t=2 mm, w=80 cm.*

The FEM was utilized to model both aluminum and iron shields for the sake of comparison. The obtained data are presented in Fig. 5. For the thickness of t=2 mm, it seems that both aluminum and iron shields are equally effective.

The MCM was used to calculate the data presented in Fig. 6 and 7. Both aluminum shield of t=4mm and aluminum shield of t=8mm offered much better field reduction than the iron plate of t=2mm. The MCM was found to be very quick, easily adaptable and convenient for repetitive detailed calculations.

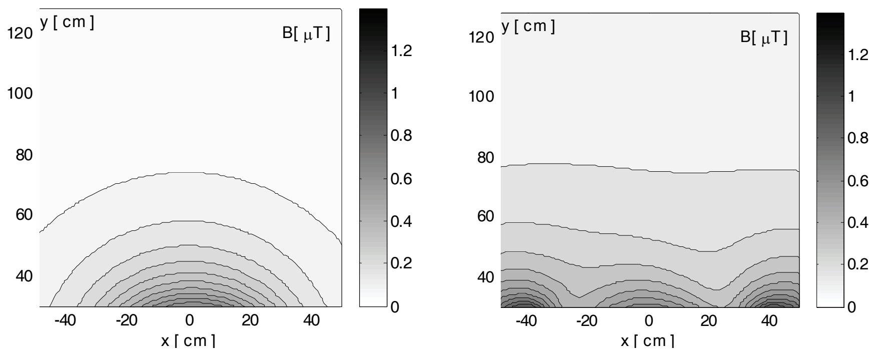

a) h = 5 cm *b) h = 25 cm*

Fig. 6 – *Vector B magnitude starting 30 cm above the three phase conductors for the different aluminum shield heights h, t=4 mm, w=80 cm.*

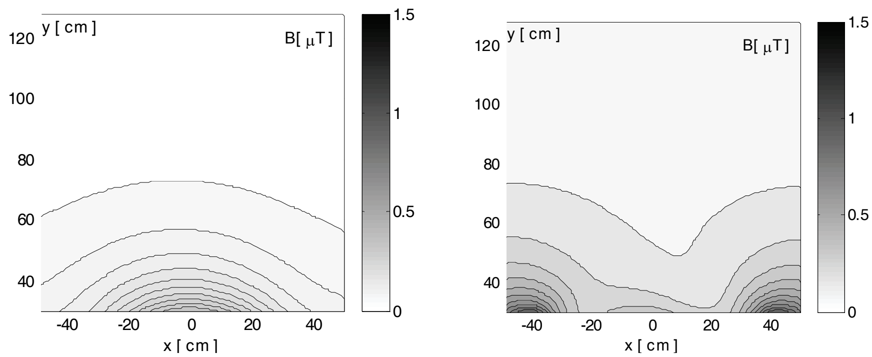

a) h = 5 cm *b) h = 25 cm*

Fig. 7 – *Vector B magnitude starting 30 cm above the three phase conductors for the different aluminum shield heights h, t=8 mm, w=80 cm.*

4 Shielding Effectiveness

Analyzing the magnetic flux density through the space above the shield it is possible to estimate its effectiveness *S*, which also can be plotted as the field reduction pattern. The shielding effectiveness in this work at any point of interest is defined as

$$S = \frac{B_{without\ the\ shield}}{B_{with\ the\ shield}} . \tag{7}$$

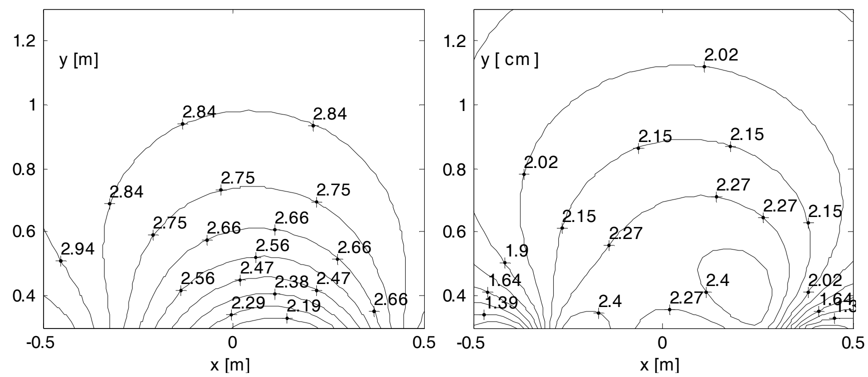

a1) Aluminum, h = 5 cm b1) Aluminum, h =25 cm

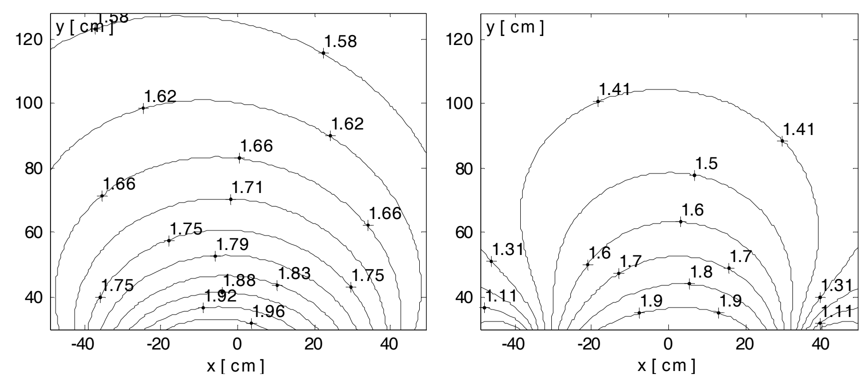

a2) Iron, h = 5 cm b2) Iron, h = 25 cm

Fig. 8 – *The shielding effectiveness for the area of interest starting 30cm above the three phase conductors for the different shield heights h; Aluminum and Iron shield, t=2mm,w=80cm.*

5 Conclusions

This work explored the shielding effectiveness of non-ferrous conductive shields. Ferrous plates were explored too for the sake of completeness and comparison. Ferrous shields are efficient only if completely surrounding the source of the field. Thick aluminum plates were analyzed by two different 2D methods: MCM and FEM. The results obtained by the two methods were in a good agreement. The FEM was applicable to both ferrous and non-ferrous shields. The MCM was limited to non-ferrous shields only. The MCM was much quicker than the FEM and provided easier data manipulation and more insight into the details of the field attenuation. Aluminum was identified as a suitable shielding material for moderate field reduction due to its low cost and satisfactory shielding performance.

In the case of non-ferrous metallic plates some key influences of the parameters were identified:

1) increasing thickness leads to improved shielding performance;

2) the shield location has a major impact on the field distribution; and

3) the shield effectiveness depends strongly on the position of the shield.

It was shown that major field reduction in the region of interest occurs if the shield is close enough to the conductors. With the shield closer to the conductors, the field is gradually reduced. As the shield moves away from the conductors, the zone of the field reduction gets more and more localized, as can be seen from Figs. 9b and 10b.

The influence of the shields' width on the shielding performance was investigated recently [5]. A wider shield was found more effective. Also a shield closer to the conductors offered more attenuation per unit area (See Figs. 6 and 7).

In most cases the field was not symmetrical in the zone of interest. This was the consequence of asymmetric induced currents in the shield, due to the different distances from the current caring conductors (See Figs. 4a and 4b). The asymmetry was not sensitive to the currents' phase shift, but was sensitive to the currents' sequence. The direct sequence currents and the reverse sequence currents gave two distinct sets of induced currents (See Fig. 4c). The field asymmetry was more pronounced when the shield was closer to the conductors (See Figs. 9 and 10).

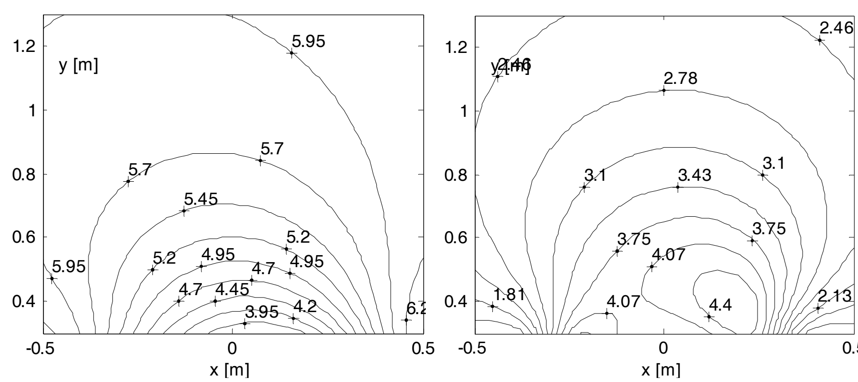

a) Aluminum, h = 5 cm   *b) Aluminum, h = 25 cm*

Fig. 9 – *The shielding effectiveness for the area of interest starting 30 cm above the three phase conductors for the different shield heights h; Aluminum shield, t=4 mm, w=80 cm.*

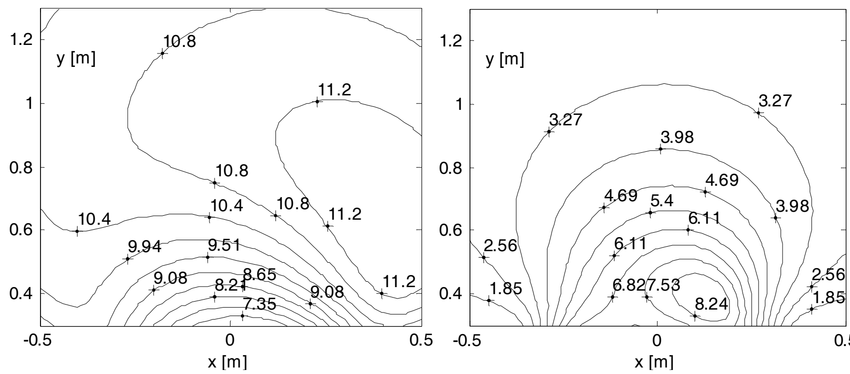

a) Aluminum, h = 5 cm *b) Aluminum, h = 25 cm*

Fig. 10 – *The shielding effectiveness for the area of interest starting 30 cm above the three phase conductors for the different shield heights h; Aluminum shield, t=8 mm, w=80 cm.*

Aluminum shield 8 mm thick was found to reduce the vector B magnitude about 11 times (Fig. 10). This is approximately the most that can be expected from an aluminum plate of reasonable thickness. Thicker shields were tested, but the improvement in the field attenuation was mild (for instance maximally 16 for a t=12mm thick shield).

From our calculations it follows that the t=4mm and t=8mm thick aluminum plates can reduce power frequency magnetic field better than the t=2mm ferromagnetic plate. Shielding principles derived in this work can be utilized in practical applications for long lines, bus bars and cables.

6 Acknowledgments

This work was partly completed under project "Modeling of the Electromagnetic Fields in Electro-distributive Systems", financed by the Ministry of Science, Technology and Development, Republic of Serbia. The project was also sponsored by EPS-Power Distribution Company of Serbia.

7 References

[1] D. R. J. White: Electromagnetic interference and compatibility, EMI Control Methods and Techniques. Germantown, MD: Don White Consultants, Inc., vol. 3, 1973, pp. 10-11.

[2] B. Popović: Elektromagnetika, Beograd: Građevinska knjiga, 1986, pp 10-11.

[3] W. M. Frix, G.G. Karady: A circuital approach to estimatethe magnetic field reduction of nonferrous metal shields, IEEE Trans. EMC Vol. 39, No.1, 1997 pp 24-32.

[4] M. Prsa, Lj. Geric, R. Obradovic, M. Jovanovic: Povrsinski efekat i efekat blizine U sabirnica, 24 savetovanje JUKO-CIGRE Vrnjacka Banja 1999, pp R23-12/01-R23-12/06.

[5] M. Milutinov, N. Pekarić-Nađ: Estimation of the network frequency magnetic field reduction by nonferrous metallic shields, PSU-UNS First International Conference on Engineering and Environment – ICEE, Novi Sad, May 2005.